AJNR

MR Imaging in the Presurgical Workup of Patients with Drug-Resistant Epilepsy

Horst Urbach, Jörg Hattingen, Joachim von Oertzen, Cordelia Luyken, Hans Clusmann, Thomas Kral, Martin Kurthen, Johannes Schramm, Ingmar Blümcke and Hans H. Schild

This information is current as of June 1, 2025.

AJNR Am J Neuroradiol 2004, 25 (6) 919-926
http://www.ajnr.org/content/25/6/919

AJNR Am J Neuroradiol 25:919–926, June/July 2004

MR Imaging in the Presurgical Workup of Patients with Drug-Resistant Epilepsy

Horst Urbach, Jörg Hattingen, Joachim von Oertzen, Cordelia Luyken, Hans Clusmann, Thomas Kral, Martin Kurthen, Johannes Schramm, Ingmar Blümcke, and Hans H. Schild

BACKGROUND AND PURPOSE: **Whether an epileptic lesion is detected with MR imaging depends on the quality of the images and the expertise of the reader. We analyzed the role of 1.5-T MR imaging in the presurgical evaluation of patients with drug-resistant epilepsy at one center.**

METHODS: **In a 2-year prospective study, 385 patients with drug-resistant epilepsy underwent standardized MR imaging at 1.5 T. We analyzed whether lesions were detected, whether they were precisely characterized by MR imaging, and whether lesion characterization allowed us to estimate seizure outcomes.**

RESULTS: **Lesions were found on MR images in 318 patients (83%). Following presurgical evaluation, 209 (66%) underwent surgery, and 109 (34%) did not. Freedom from seizures was achieved in 130 (70%) of 186 patients. Nine (14%) of 66 patients without an MR imaging lesion underwent surgery; histopathologic findings were unrevealing in seven patients, and five (56%) achieved freedom from seizures. Hippocampal sclerosis was the most common lesion (52%) and correctly characterized in 101 (97%) of 104 patients. Glioneuronal tumors (20%) were sometimes imprecisely characterized: Four nonenhancing gangliogliomas were mistaken for focal cortical dysplasias. Outcomes were not different between lesion groups. However, there were trends toward a favorable outcome for focal cortical dysplasias with balloon cells and an unfavorable outcome for gyral scars.**

CONCLUSION: **MR imaging detection of lesions influences further presurgical workup, though lesion characterization does not allow us to predict seizure outcome. If MR imaging fails to depict a lesion and patients undergo surgery because of electrophysiologic findings, histopathologic findings are often unrevealing.**

MR imaging has become one of the most important tools in the selection of patients with drug-resistant focal epilepsy for surgery. Congruity of an MR imaging lesion, ictal epileptic EEG discharges, and seizure semiology may allow for epilepsy surgery without further invasive diagnostic procedures. In patients, in whom scalp EEG recordings are insufficient, a lesion depicted at MR imaging may generate a hypothesis for intracranial electrode implantation.

Whether a lesion is detected with MR imaging depends on the quality of the images and the expertise of the reader (1). To detect a lesion, most epilepsy centers acquire high-resolution MR images on 1.5-T systems by using standardized protocols that consider seizure semiologic and EEG findings.

In the present study, we investigated the MR imaging protocol of the epilepsy center at the University of Bonn, Germany. This protocol was implemented after a new 1.5-T system had been installed. We investigated the accuracy of this protocol by addressing the following questions: 1) How many and which lesions are detected in patients with drug-resistant focal epilepsy? 2) Are the lesions correctly characterized with MR imaging? 3) Does the seizure outcome following surgery depend on the type of lesion shown at MR imaging?

Received August 4, 2003; accepted after revision November 8.

From the Departments of Radiology (H.U., J.H., H.H.S.), Epileptology (J.v.O., M.K.), Neurosurgery (C.L., H.C., T.K., J.S.), and Neuropathology (I.B.), University of Bonn Medical Center, Germany.

Address reprint requests to Horst Urbach, MD, Department of Radiology/Neuroradiology, University of Bonn Medical Center, Sigmund Freud Str 25, D - 53105 Bonn, Germany.

© American Society of Neuroradiology

Methods

Study Group

The study group comprised all patients with drug-resistant focal epilepsies who were admitted to the Department of Epileptology at the University of Bonn for presurgical evaluation between January 1999 and December 2000.

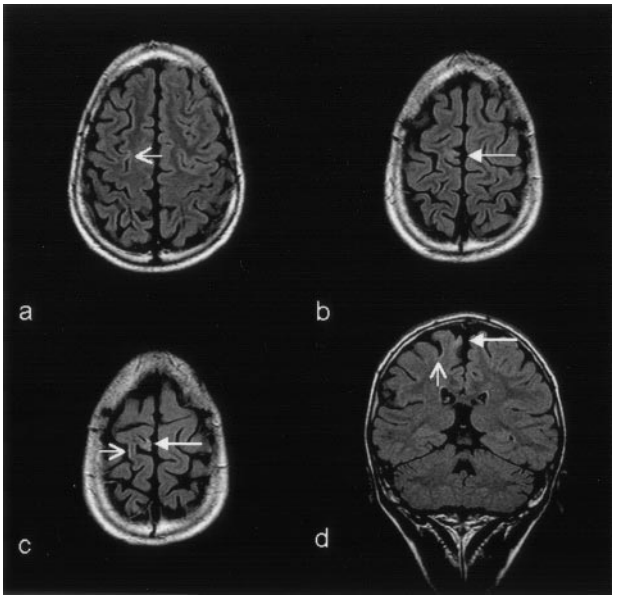

FIG 1. Scarring of the left superior frontal gyrus. Axial 5-mm-thick (*a–c*) and coronal 3-mm-thick (*d*) FLAIR fast spin-echo images show an atrophic and hyperintense lesion in the right superior frontal gyrus (*solid-head arrows* in *a–d*). Note also a tiny increase in signal intensity and the atrophy in the depth of the right frontal superior sulcus (*open-head arrows* in *a*, *c*, and *d*)

MR Imaging

MR imaging was performed by using a 1.5-T system (Gyroscan ACS-NT; Philips Medical Systems). First, we performed a 3D T1-weighted gradient-echo sequence in the sagittal orientation. Section thickness was 1.1 mm. With a FOV of 250 mm, a rectangular FOV of 84%, a matrix of 256 × 256, and 179 phase-encoding steps, roughly isotropic voxels (1.17 × 1.17 × 1.1 mm) resulted. Displaying the sagittal 3D T1-weighted gradient-echo sequence, the next two sequences, an axial fluid-attenuated inversion recovery (FLAIR) fast spin-echo and an axial T2-weighted fast spin-echo sequence with a section thickness of 5 mm and a intersection gap of 1 mm were angulated either along the length-axis of the hippocampus or the anterior commissure–posterior commissure (AC-PC). How the sections were angulated depended on seizure semiologic and EEG findings and was decided after patient history was reported from the transferring epileptologist (J.V.O., M.K.). In most patients, sections were angulated along the length-axis of the hippocampus. If seizure semiologic or EEG findings, or both indicated the primary motor or sensory cortex or the dorsal frontal lobe (Fig 1), sections were angulated along the AC-PC line. MR imaging was continued with coronal FLAIR fast spin-echo (section thickness, 3 mm), coronal T2-weighted fast spin-echo (section thickness, 2 mm), and coronal T1-weighted inversion recovery sequences (section thickness, 5 mm; intersection gap, 0.5 mm). If axial sequences were angulated along the hippocampal length-axis, section orientation was perpendicular to axial sections. If axial sequences were angulated along the AC-PC line, the coronal FLAIR sequence was tilted along the brain stem, but the coronal T2-weighted sequence was perpendicular on hippocampal length axis.

If a lesion other than hippocampal sclerosis was detected, axial and/or coronal T1-weighted spin-echo sequences (section thickness of 5 mm, intersection gap of 1 mm) before and following the injection of gadopentetate dimeglumine were performed.

Further Presurgical Workup

Results of further presurgical work-up, as reported in each patient, was analyzed. These included stereo-EEG monitoring in all patients. Other investigations (ictal and interictal single photon emission CT [SPECT], subtraction ictal SPECT co-registered to MR imaging [SISCOM; Siscom Inc., Dayton, OH], positron emission tomography, depth electrodes, subdural grid or strip electrode study) were performed as deemed necessary in each patient.

Surgery and Postsurgical Outcome

We analyzed surgical approaches as targeted to resect or disconnect the epileptogenic zone while sparing eloquent cortical areas. All surgical patients were reexamined at routine intervals of 3 months, 6 months, and 1 year following surgery. Seizure outcome was determined according to the classification by Engel et al (2).

Histopathology

Surgical specimens submitted for neuropathologic evaluation were microscopically analyzed by using hematoxylin-eosin, hematoxylin-eosin Luxol fast blue, and Nissl staining. Immunohistochemical studies included reactions with a monoclonal antibody directed against Vimentin (V9, Dako, Hamburg, Germany), polyclonal antibodies directed against glial fibrillary acid protein, a monoclonal antibody directed against human neurofilament protein (2F11, Dako), a monoclonal antibody directed against neuronal specific enolase, a monoclonal antibody to synaptophysin (SY 38, Dako), a monoclonal antibody directed against Ki67 (MIB1, Dako), and a monoclonal antibody directed against CD 34 (QBend 10, Immunotech; Medicorp Inc., Montreal, PQ, Canada) by using standard protocols and the avidin-biotin-peroxidase complex with diaminobenzidine as chromogen (12).

Image Evaluation

A single reader (H.U.) reviewed all MR images. If a lesion was found, the reader attempted a histopathologic diagnosis. MR imaging reports, as detailed within 1 week after the examination, were collected by an independent examiner (J.H.) in a computerized database and compared with the final histopathologic diagnosis.

Statistical Analysis

Statistical analysis was performed when appropriate. In group comparisons, Fisher exact tests or, in larger groups, χ^2 tests were performed. The significance level was set at $P = .05$.

Results

Study Group

Within the 2-year period, 385 patients were included (207 male, 178 female). Their mean age was 31 years (range, 8 months to 67 years). The patients had drug-resistant focal epilepsy for 8 months to 42 years.

MR Imaging, Surgical, and Postsurgical Outcomes

MR imaging revealed lesions in 318 (83%) of 385 patients (Fig 2, Table 1). Following further presurgical work up, 209 (66%) of 318 patients underwent surgery, and 109 patients (34%) did not. Of these 109 patients, 42 patients did not undergo surgery, because MR imaging showed diffuse bilateral or multifocal lesions. In 39 patients, surgery was not recommended because lesions affected the eloquent cortex ($n = 19$),

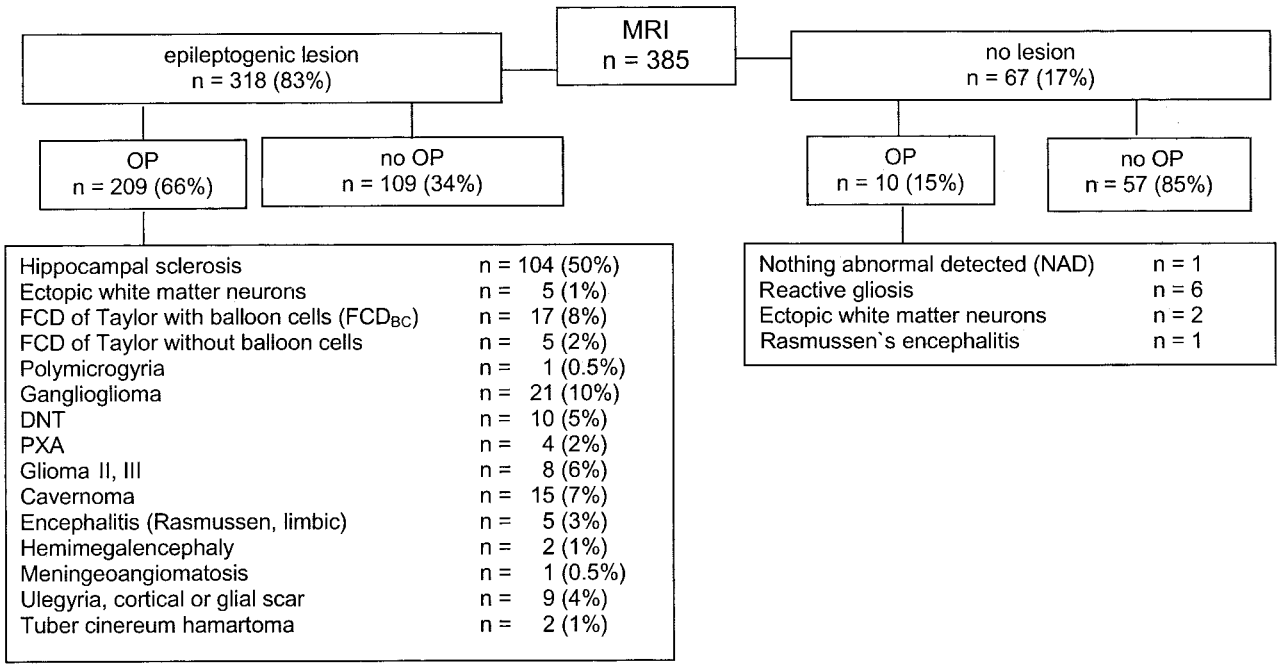

FIG 2. Schematic depiction of method used in MR imaging lesion detection.

TABLE 1: MR lesion type and seizure outcome

		Outcome/Engel IA Class
MR with lesion		
Hippocampal sclerosis	104 (50%)	65 /93 (70%)
Ectopic white matter neurons	3 (1%)	2 /3 (66%)
FCD with balloon cells	17 (8%)	13 /16 (81%)
FCD without balloon cells	5 (2%)	2 /4 (50%)
Polymicrogyria	1 (0.5%)	0 /1 (0%)
Ganglioglioma	21 (10%)	15 /21 (71%)
DNT	10 (5%)	7 /9 (78%)
PXA	4 (2%)	3 /3 (100%)
Glioma II, III	8 (6%)	6 /7 (86%)
Cavernoma	15 (7%)	11 /15 (73%)
Hemimegalencephaly	2 (1%)	1 /2 (50%)
Meningeoangiomatosis	1 (0.5%)	1 /1 (100%)
Ulegyria, cortical, or glial scar	9 (4%)	3 /9 (33%)
Tuber cinereum hamartoma	2 (1%)	1 /2 (50%)
MR without lesion		
NAD	1	0 /1
Reactive gliosis	6	3 /6
Ectopic white matter neurons	2	2 /2

Note.—NAD indicates nothing abnormal detected.

the likelihood of a significant reduction in seizures was low ($n = 12$), or the epileptogenicity of the lesion could not be proved ($n = 8$). In five patients, seizures were markedly reduced with modified antiepileptic drug therapy. Twenty-one patients refused surgery because their perspective likelihood of achieving freedom from seizure was low, and two patients died before surgery could be performed.

MR imaging did not depict lesions in 67 patients (17%). Nine patients in this cohort (14%) underwent surgery, because seizure semiology and EEG recordings from intrahippocampal-depth and temporobasal and lateral strip electrodes indicated that the ictal-onset zone was within one temporal lobe. One patient with epilepsia partialis continua underwent brain biopsy in the postcentral gyrus; the results revealed Rasmussen encephalitis.

Outcomes were available for 186 of 209 surgical patients with MR imaging signs of lesions and for all nine patients without MR imaging signs of lesions (five patients who underwent biopsy were excluded from this calculation). One year following surgery, 130 patients in the lesion group and five patients in the nonlesion group were seizure free (Engel class IA; P .05, Fisher exact test).

MR Imaging and Histopathologic Analysis

MR imaging readings and histopathologic diagnoses are detailed in Table 2. A total of 104 patients had histologically proved sclerosis of the Ammon horn sclerosis: 85 patients with well-preserved hippocampi in which the different segments of CA1-CA4, the dentate gyrus, and the subiculum could be analyzed and 19 patients with specimens sufficient to assess neuron loss in either CA1 or CA3 and CA4. Of these, 101 patients had MR findings of increased signal intensity and a reduced size of the resected hippocampus and subseqently were considered to have hippocampal sclerosis. Three patients had atrophic hippocampi with normal signal intensity on coronal T2-weighted images and were not considered to have hippocampal sclerosis. Reduced gray matter–white matter demarcation of the temporal pole on coronal T2-weighted images was seen in 18 of 104 patients. Because 96 patients were treated with selective amygdalohippocampectomy and only eight of 104 patients underwent anterior two-thirds temporal lobectomy, the histopathologic substrate of reduced gray matter–white matter demarcation of the tempo-

TABLE 2: Lesion type and MR diagnosis

Histopathologic Findings	MR Findings
Hippocampal sclerosis	101 hippocampal sclerosis, 3 atrophy, no sclerosis
Ectopic white matter neurons	2 poor gray-white matter demarcation, 1 FCD without BC, 2 NAD
FCD with balloon cells (FCD_{BC})	14 FCD_{BC}, 2 cortical/glial scar, 1 equivocal findings
FCD without balloon cells	3 FCD without BC, 2 ganglioglioma
Polymicrogyria	1 Polymicrogyria
Ganglioglioma	16 ganglioglioma, 4 FCD without BC, 1 DNT
DNT	8 DNT, 1 ganglioglioma, 1 FCD without BC
PXA	1 PXA, 3 ganglioglioma
Glioma II, III	5 glioma, 2 ganglioglioma, 1 limbic encephalitis
Cavernoma	15 cavernoma
Enzephalitis (Rasmussen, limbic)	5 encephalitis, 1 NAD
Hemimegalencephaly	2 hemimegalencephaly
Meningeoangiomatosis	1 ganglioglioma
Ulegyria, cortical, or glial scar	7 cortical/glial scar, 1 ganglioglioma, 1 DNT
Tuber cinereum hamartoma	2 tuber cinereum hamartoma
Reactive gliosis	6 NAD
Normal	1 NAD

Note.—NAD indicates nothing abnormal detected.

ral pole remains unclear. Two patients had sclerosis of the Ammon horn plus ectopic white matter neurons in the temporal pole, whereas in six patients, sclerosis of the Ammon horn was the only pathologic finding. Neuropathologically, ectopic white matter neurons without sclerosis of the Ammon horn was found in five patients. MR images in two patients showed reduced gray matter–white matter demarcation of the temporal pole, as indicative of ectopic white matter neurons. Two patients had normal MR images, and in one patient with inhomogeneity of the corpus amygdaloideum, focal cortical dysplasia was suspected.

Focal cortical dysplasia of the Taylor balloon cell type (FCD_{BC}) was the histopathologic diagnosis in 17 patients. It was considered correct in 14 patients. In two patients, tissue was atrophic and gyral scarring was suspected, and one patient had no clear-cut MR imaging diagnosis (Fig 3). Focal cortical dysplasia without Taylor balloon cells was the histopathologic diagnosis in five lesions. With MR imaging, two of these lesions were considered gangliogliomas.

One focal polymicrogyria with small gyri and a focally enlarged subarachnoid space was diagnosed correctly. This lesion exhibited a normal signal intensity of the cortex and the subcortical white matter on T2-weighted and FLAIR images and was best visualized on reformatted planar surface views (Fig 4).

Sixteen of 21 gangliogliomas of World Health Organization (WHO) grade I were diagnosed correctly; four were mistaken for focal cortical dysplasias, and one was mistaken for a dysembryoplastic neuroepithelial tumor (DNT). Eight of 10 DNTs were diagnosed correctly, while one DNT was confused with a ganglioglioma, and another DNT was confused with a focal cortical dysplasia without Taylor balloon cells. Although three pleomorphic xanthoastrocytoma (PXAs) had typical imaging findings (one did not), two lesions were mistaken for gangliogliomas (Fig 5). Two of eight astrocytomas were considered gangliogliomas, while one limbic astrocytoma was considered limbic encephalitis (Fig 6).

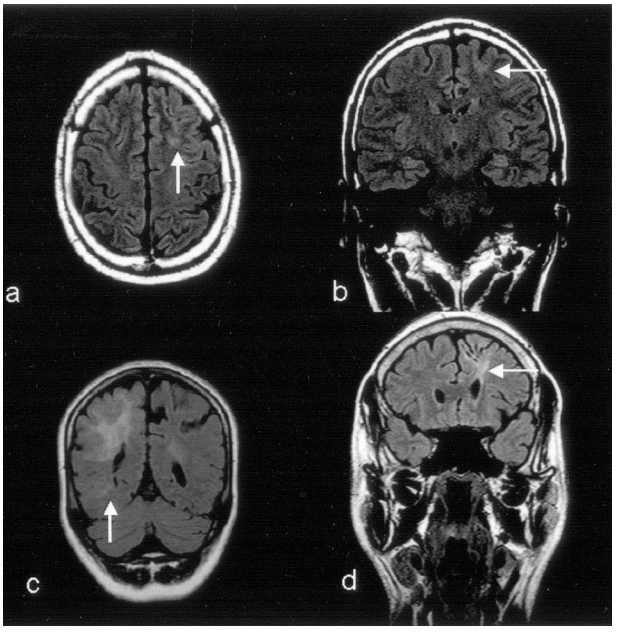

FIG 3. Focal cortical dysplasia of the Taylor balloon cell type (FCD_{BC}). Images in *a* and *b* show a small lesion in the depth of the left frontal superior sulcus (*arrow*). Image in *c* shows a huge lesion and a small lesion (*arrow*) in the right parietal and occipital lobe. Image in *d* shows a lesion under an atrophic left superior frontal gyrus. The MR imaging hallmark of FCD_{BC} is a subcortical hyperintensity tapering toward the lateral ventricle. It is clearly visible (*arrow*), but because of atrophy of the superior frontal gyrus, the lesion was mistaken for gyral scarring.

All 15 cavernomas were diagnosed correctly. Thirteen cavernomas exhibited a reticulated core of mixed signal intensity on T1-weighted spin-echo and T2-weighted fast spin-echo images; this was surrounded by a hypointense rim on T2-weighted fast spin-echo images (type II according to the classification by Zabramski et al [3]). Two cavernomas had a hyperintense core on T1- and T2-weighted images sur-

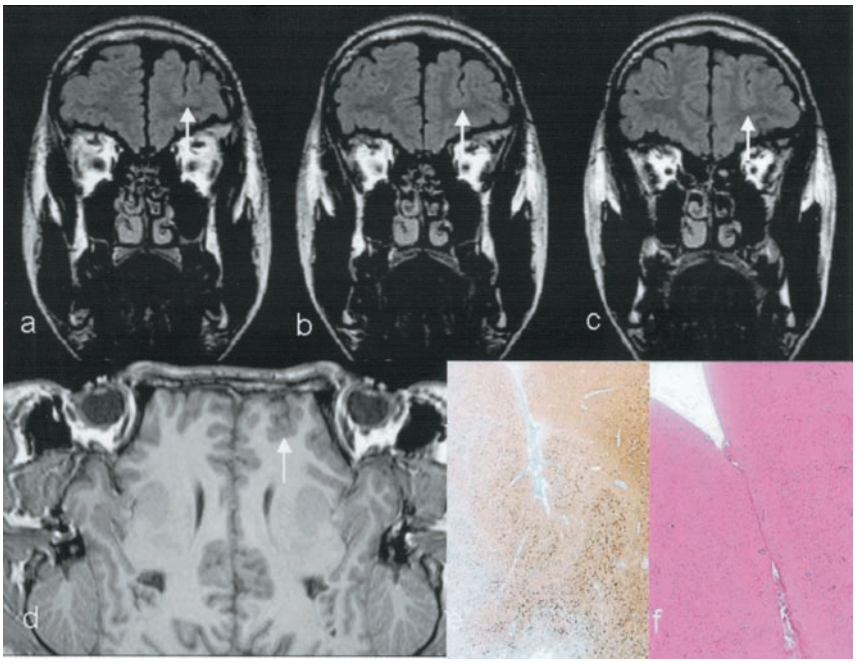

FIG 4. Focal polymicrogyria in the left frontal lobe. Contiguous, 3-mm-thick, coronal FLAIR fast spin-echo sections (*a–c*) show a deep superior frontal sulcus with a slightly irregular contour and a normal signal intensity of the cortex (*arrow*). Planar surface-reconstructed view (*d*) generated from a 1.1-mm-thick, 3D, T1-weighted gradient-echo sequence confirms the distorted anatomy (*arrow*). Histopathologic sections show loss of neocortical architecture (MAP2 [*e*]) compared with that of adjacent six–layered cortex (nematoxylin–eosin straining [*f*]).

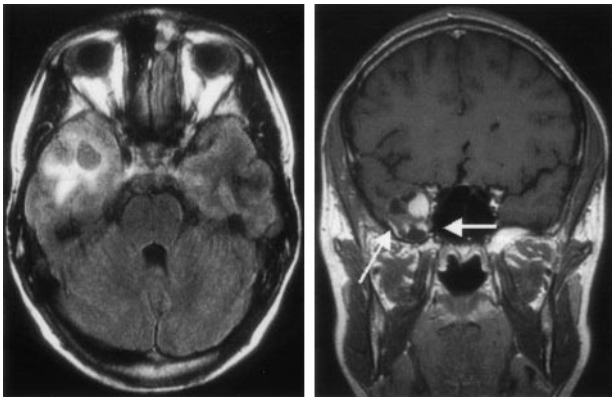

FIG 5. PXA of the right temporal lobe. The lesion shows typical meningeocerebral contrast enhancement (*arrows*), cystic parts, and surrounding edema.

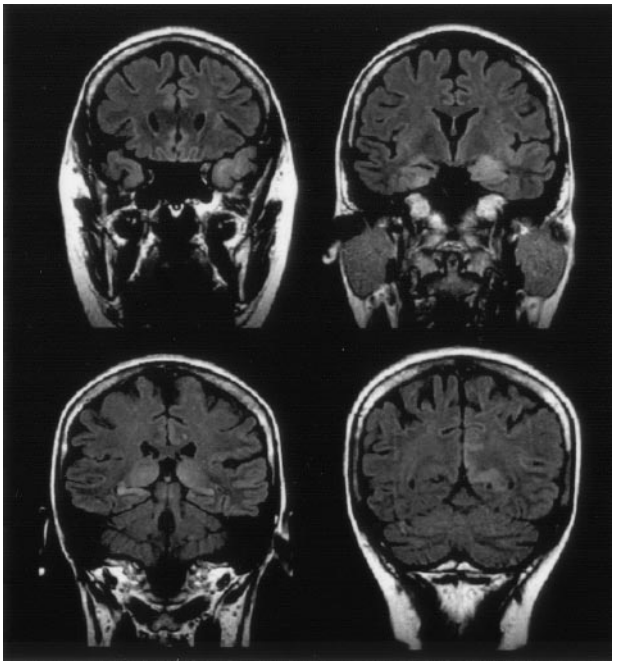

FIG 6. Anaplastic (limbic) astrocytoma of WHO grade III. Coronal 3-mm-thick FLAIR fast spin-echo sections show increased volume and signal intensity of both temporopolar cortices, the amygdala, hippocampi, thalami, and left parietal cortex. Because repeated CSF investigation showed a slightly increased protein content (54–95 mg/dL) and 6–8 cells per microliter, limbic encephalitis was suspected.

rounded by a hypointense rim in one patient and a small hyperintense zone suggesting edema in the other patient. These cavernomas were classified as type I lesions with signal-intensity characteristics most likely due to subacute hemorrhage surrounded by a rim of hemosiderin-stained macrophages and gliotic brain (3). One patient had two cavernomas interconnected by a hypointense band, and another patient had three independent cavernomas. Once the cavernoma was detected with MR imaging, the patients underwent T2*-weighted gradient-echo imaging, which revealed larger hypointense peripheral zones but no further cavernomas.

Five of six cases of Rasmussen or limbic encephalitis were diagnosed correctly. However, in one 13-year-old female adolescent with epilepsia partialis continua and motor seizures of the right side, biopsy of the left superior frontal gyrus revealed Rasmussen encephalitis, although MR images were normal.

Hemimegalencephaly was diagnosed with MR imaging in two patients. In both, functional hemispherotomy with removal of the frontal operculum, uncus, amygdala, and hippocampus was performed. The results showed dysplastic neurons and balloon cells suggestive of hemimegalencephaly (4).

One girl had meningeoangiomatosis, but this entity was not considered, and it was mistaken for a ganglioglioma. Cortical or glial scars or both were present in

nine patients (Fig 1). One lesion each was thought to be a ganglioglioma or a DNT. In two patients, tuber cinereum hamartomas was diagnosed correctly.

Nine patients with normal MR imaging findings underwent surgery after intrahippocampal-depth and temporobasal and lateral-strip electrodes indicated an ictal-onset zone within one temporal lobe. Histopathologic evaluation revealed reactive gliosis in six patients, and ectopic white matter neurons in two patients; one specimen was considered normal.

Outcome and Histopathologic Findings

Outcome analysis with respect to different histopathologic lesions and lesion groups (Ammon horn sclerosis, tumors, cortical dysplasias, other) did not show significant differences (Fisher exact tests) (Table 1). However, there were trends toward a better outcome for focal cortical dysplasias of the Taylor balloon cell type and for a worse outcome for gyral scars.

Discussion

To our knowledge, this is the largest prospective study of the role of MR imaging in the presurgical workup of patients with drug-resistant (focal) epilepsies. We found lesions in 83% of patients. However, this number must be interpreted with caution, because a considerable number of patients were transferred with MR images already displaying a lesion, indicating that preselection for presurgical workup had occurred. Our lesion-detection rate with MR imaging was comparable to that of other studies (5); it depended not only on patient selection but also on the quality of the MR images and the experience of the reader. In a former study, we showed that the lesion-detection rate was 50% with standard MR imaging but 91% if patients were examined with an epilepsy-dedicated protocol and if experienced neuroradiologists read the images (1). Two-thirds of patients with lesions in this study finally underwent surgery, and 70% were seizure-free (Engel class IA) at 1 year following surgery. If MR imaging failed to show a lesion, only 14% of patients finally underwent surgery. All these patients had anterior temporal-lobe resections, and five (56%) of nine patients were seizure-free at 1 year following surgery. The small number of surgical patients without MR imaging lesions prevented group comparisons. However, it also indicated that patients rarely undergo surgery if MR imaging does not show a lesion. This is clearly because the MR imaging detection of a lesion points to the epileptogenic zone and generates a hypothesis for further presurgical workup.

Are the lesions correctly characterized with MR imaging?

The most common histopathologic diagnosis in this study was hippocampal sclerosis. It was correctly characterized in 101 (97%) of 104 patients. In three patients, the hippocampus was atrophic, but T2-weighted fast spin-echo images showed no increased signal intensity. Although all hippocampal segments (CA1-CA4, dentate gyrus, subiculum) were not preserved in 19 of 104 specimens, we assessed these specimens as hippocampal sclerosis, because either the CA1 or the CA3 and CA4 segments showed distinct neuronal loss. In the literature, the detection rate of hippocampal sclerosis was 61–98% with visual assessment (6–13). The suggestion that T2 relaxometry increases sensitivity (7) was not supported in a former study, although T2 relaxometry is useful to prove concomitant involvement of the contralateral hippocampus, and the results are correlated with the severity of neuron loss (14). Considering the terms *sensitivity* and *specificity*, one should be aware that both cannot be calculated. Patients with negative MR imaging findings, which could represent false-negative results, usually do not undergo surgery. Also, many patients with MR imaging lesions do not undergo surgery for various reasons (34% in our series, Fig 7). This group of patients could include false-positive cases.

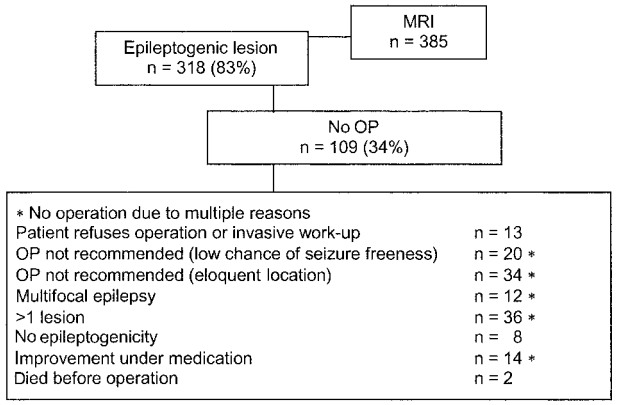

FIG 7. Schematic diagram depicting reasons not to operate on patients with MR imaging lesions.

A second large lesion group comprised patients with epilepsy-associated tumors. Sixteen of 21 gangliogliomas and eight of 10 DNTs were correctly diagnosed on the basis of MR imaging findings. Four gangliogliomas and one DNT (all nonenhancing lesions) were mistaken for focal cortical dysplasias, and one ganglioglioma and DNT each was mismatched with a DNT and a ganglioglioma, respectively. Gangliogliomas were more frequent than DNTs; this finding is in contrast to that of Pasquier et al (15), who reported 61 DNTs and 29 gangliogliomas among 327 consecutive resections from patients with drug-resistant epilepsy. These authors also described mixed tumor components in the same specimen and found a large proportion of tumors difficult to classify. Their data also support the hypothesis of a close histogenic relationship with a putative common origin from pluripotential progenitor CD34 positive cells of the subpial granular layer (15–18). There were four PXAs in our series: three had typical imaging features with a meningeocerebral contrast enhancement on T1-weighted images and white matter edema on T2-weighted and FLAIR images. Two tumors were sim-

ply mistaken for gangliogliomas, likely due to the rare occurrence of PXAs. The same holds true for a case of a meningeoangiomatosis, which showed leptomeningeal contrast enhancement and a partly calcified mass lesion at MR imaging. Among eight gliomas (two astrocytomas of WHO grade II, two astrocytomas of WHO grade III, three oligodendrogliomas of WHO grade II, and one oligodendroglioma of WHO grade III), two WHO grade II astrocytomas were mistaken for gangliogliomas, and one anaplastic astrocytoma WHO grade III was considered a limbic encephalitis due to a multifocally increased cortical signal intensity (19).

Another lesion group comprised focal cortical dysplasias. We consider this as an umbrella term for a variety of lesions resulting from disturbances of normal cortical development (20–23). Unfortunately, the nomenclature is not uniform, and different terms are used for lesions that appear identical on histologic specimens. In this series, at least the focal cortical dysplasia of the Taylor balloon cell type (FCD_{BC}), or, FCD type IIb (22), appeared as a distinct entity with respect to its MR imaging and histopathologic features. On FLAIR MR imaging, FCD_{BC} exhibited a markedly hyperintense funnel-shaped area in the subcortical white matter. Histopathologically, dysplastic neurons in the cortex and adjacent hypomyelinated white matter and accumulation of balloon cells within the hypomyelinated white matter were found (24–25). In accordance with Barkovich and coworkers (21), we found similar histopathologic findings in two patients with hemimegalencephaly treated with functional hemispherectomy including the removal of the frontal operculum, uncus, amygdala, and hippocampus (4).

Focal cortical dysplasia without balloon cells was a rare finding. Four of these lesions were in the temporal lobe, and another lesion was located in the frontal lobe. There is an ongoing discussion about the classification, especially with respect to the temporal pole lesions (20–23). We assigned a lesion in the temporal pole as a focal cortical dysplasia without balloons cells if the surgical specimen contained dysplastic neurons. At MR imaging, these lesions were not confined to the gray matter and showed focally increased signal intensity in the white matter on T2-weighted and FLAIR images. They could not be safely separated from lesions containing either clusters of ectopic neurons or single ectopic neurons with density of more than 20 per square millimeter in the white matter of the temporal pole. Ectopic white matter neurons showed widespread, increased white matter signal intensity on T2-weighted and FLAIR images in two patients but also normal MR imaging results in two other patients.

One patient in this series had histologically proved focal polymicrogyria that appeared as focal lesion with small gyri exhibiting a normal signal intensity of the cortex and the subcortical white matter on T2-weighted and FLAIR images. Some consider focal polymicrogyria a focal cortical dysplasia (20–21), and other authors do not list the condition under this umbrella term (22–23).

Most cavernomas in this study were type II cavernomas according to the classification by Zabramski et al (3) and readily appreciated on T2-weighted fast spin-echo images. Nevertheless, if a cavernoma was suspected on the basis of MR imaging findings, we additionally acquired T2*-weighted gradient-echo images, which did not depict any further cavernomas in this series. Type II cavernomas have signal intensity characteristics indicating loculated areas of hemorrhage and thrombosis of varying age and large areas of hemosiderin-stained brain. These cavernomas are known to cause seizures due to progressive hemosiderin deposition within the brain surrounding the cavernoma. Type II cavernomas are more likely to cause seizures than are type III or type IV cavernomas, which may develop de novo and which are often asymptomatic (3).

The imaging findings of Rasmussen and limbic encephalitis have been described in detail (26–27). A prodromal or acute state with a swollen cortex is rarely observed with MR imaging (26). Most patients, and five of six patients in this 2-year series, presented with an already atrophic cortex. One patient had normal MR images, which is an unusual finding in Rasmussen encephalitis.

Gyral scars have a characteristic MR imaging pattern with a focally widened subarachnoid space and a hyperintense and atrophic cortex on long-TR, long-TE sequences. Because of nulling of the CSF signal intensity, this pattern is best appreciated on FLAIR MR images perpendicular to the brain surface. The patient's history supports the diagnosis of gyral scarring: three of our nine patients had meningitis in early childhood, and another three patients had a history of birth injury. For many patients who had birth injuries and other hypoxic-ischemic events in early childhood, FLAIR MR imaging shows the depths of the parieto-occipital sulci that are heavily affected, leaving pedunculated gyri on long stalks. Ulegyria is the appropriate term for this condition, and because this is usually a bilateral disease, patients are rarely surgical candidates (28).

Does the seizure outcome after surgery depend on the type of the MR imaging lesion?

The goal of epilepsy surgery is to remove or disconnect the epileptogenic zone defined as area of cortex indispensable for the generation of seizures (29). The epileptogenic zone is a theoretic construct, but it may be congruent with the ictal onset zone, which is defined as area of cortex from which the seizures are actually generated (29). At our institution, ictal-onset zone and eloquent cortex are often determined with intrahippocampal-depth, measurement, subdural grid, or strip electrodes, resulting in resections that are usually larger than the lesions themselves (30–31). Therefore, the question of whether seizure outcome depends on the lesion type cannot be answered accurately. In this study, seizure outcomes were not different between different lesion groups. However, some lesions tended to have a bet-

ter outcome. Focal cortical dysplasias of FCD_{BC} obviously have a good outcome (80% or more) (15, 24, 32). This may be due to several facts: FCD_{BC} lesions are precisely characterized by MR imaging (24), they have a high epileptogenicity (33) so the ictal-onset zone can easily be determined, and they are genetically determined lesions suggesting a genomic heterogeneity between lesions and normal brain tissue (25). On the other end of the spectrum, gyral scars were associated with an unfavorable outcome (33%), which may be explained by the fact that these are acquired and more widespread lesions, and MR imaging may show only some findings (Fig 1).

Conclusion

The MR imaging depiction of a lesion influences a patient's further presurgical workup. However, the precise characterization of lesion does not allow us to predict seizure outcomes following surgery. If MR imaging fails to depict a lesion and patients undergo surgery on the basis of EEG findings, histopathologic findings are often unrevealing.

References

1. von Oertzen J, Urbach H, Jungblut S, et al. **Standard MRI is inadequate for patients with refractory focal epilepsy.** *J Neurol Neurosurg Psychiatry* 2002;73:643–647
2. Engel J Jr, Van Ness PC, Rasmussen TB, Ojemann LM. **Outcome with respect to epileptic seizures.** In: Engel J Jr, ed. *Surgical Treatment of the Epilepsies.* New York: Raven Press, 1993;609–621
3. Zabramski JM, Wascher TM, Spetzler RF, et al. **The natural history of familial cavernous malformations: results of an ongoing study.** *J Neurosurg* 1994;80:422–432
4. Schramm J, Kral T, Clusmann H. **Transsylvian keyhole functional hemispherectomy.** *Neurosurgery* 2001;49:891–900
5. Siegel AM, Jobst BC, Thadani VM, et al. **Medically intractable localization-related epilepsy with normal MRI: presurgical evaluation and surgical outcome in 43 patients.** *Epilepsia* 2001;42:883–888
6. Brooks BS, King DW, Gammal T, et al. **MR imaging in patients with intractable complex partial seizures.** *AJNR Am J Neuroradiol* 1990;11:93–99
7. Jackson GD, Berkovic SF, Tress BM. **Hippocampal sclerosis can be reliably detected by magnetic resonance imaging.** *Neurology* 1990; 40:1869–1875
8. Garcia PA, Laxer KD, Barbaro NM, Dillon WP. **Prognostic value of qualitative magnetic resonance imaging hippocampal abnormalities in patients undergoing temporal lobectomy for medically refractory seizures.** *Epilepsia* 1994;35:520–524
9. Grünewald RA, Jackson GD, Connely A, Duncan JS. **MR detection of hippocampal disease in epilepsy: factors influencing T2 relaxation time.** *AJNR Am J Neuroradiol* 1994;15:1149–1156
10. Kuzniecky RI, Bilir E, Gilliam F, et al. **Multimodality MRI in mesial temporal sclerosis: relative sensitivity and specificity.** *Neurology* 1997;49:774–778
11. Bronen RA, Fulbright RK, King D, et al. **Qualitative MR imaging of refractory temporal lobe epilepsy requiring surgery: correlation with pathology and seizure outcome after surgery.** *AJR Am J Roentgenol* 1997;169:875–882
12. Meiners LC, Witkamp TD, Kort GAP, et al. **Relevance of temporal lobe white matter changes in hippocampal sclerosis.** *Invest Radiol* 1999;34:38–45
13. Eriksson S, Malmgren K, Rydenhag B, Jönsson L, Uvebrant P, Nordborg C. **Surgical treatment of epilepsy - clinical, radiological and histopathological findings in 139 children and adults.** *Acta Neurol Scand* 1999;99:8–15
14. von Oertzen J, Urbach H, Bluemcke I, et al. **Time-efficient relaxometry of the entire hippocampus is feasible in temporal lobe epilepsy.** *Neurology* 2002;58:257–264
15. Pasquier B, Peoc'H M, Fabre-Boquentin B, et al. **Surgical pathology of drug-resistant partial epilepsy. A 10-year-experience with a series of 327 consecutive patients.** *Epileptic Disord* 2002;4:99–119
16. Blümcke I, Giencke K, Wardelmann E, et al. **The CD34 epitope is expressed in neoplastic and malformative lesions associated with chronic, focal epilepsies.** *Acta Neuropathol* 1999;97:481–490
17. Blümcke I, Wiestler OD. **Gangliogliomas: an intriguing tumor entity associated with focal epilepsies.** *J Neuropathol Exp Neurol* 2002;61:575–584
18. Luyken C, Blümcke I, Fimmers R, et al. **The spectrum of long-term epilepsy associated tumors: long-term seizure and tumor outcome and neurosurgical aspects.** *Epilepsia* 2003;44:822–830
19. Bien CG, Schulze-Bonhage A, Deckert-Schlüter M, et al. **Limbic encephalitis unrelated to neoplasm as a cause of temporal lobe epilepsy.** *Neurology* 2000;55:1823–1828
20. Mischel PS, Nguyen LP, Vinters HV. **Cerebral cortical dysplasia associated with pediatric epilepsy: review of neuropathologic features and proposal for a grading system.** *J Neuropathol Exp Neurol* 1995;54:137–153
21. Barkovich AJ, Kuzniecky RI, Jackson GD, Guerrini R, Dobyns WB. **Classification system for malformations of cortical development: update 2001.** *Neurology* 2001;57:2168–2178
22. Palmini A, Lüders H. **Classification issues in malformations caused by abnormalities of cortical development.** *Neurosurg Clin N Am* 2002;13:1–16
23. Tassi L, Colombo N, Garbelli R, et al. **Focal cortical dysplasia: neuropathological subtypes, EEG, neuroimaging and surgical outcome.** *Brain* 2002;125:1719–1732
24. Urbach H, Scheffler B, Heinrichsmeier T, et al. **Focal cortical dysplasia of Taylor's balloon cell type: a clinicopathological entity with characteristic neuroimaging and histopathological features, and favorable postsurgical outcome.** *Epilepsia* 2002;43:33–40
25. Becker AJ, Urbach H, Scheffler B, et al. **Focal cortical dysplasia of Taylor's balloon cell type: Mutational analysis of the TSC1 gene indicates a pathogenic relationship to tuberous sclerosis.** *Ann Neurol* 2002;52:29–37
26. Bien CG, Urbach H, Deckert M, et al. **Diagnosis and staging of Rasmussen's encephalitis by serial MRI and histopathology.** *Neurology* 2002;58:250–257
27. Bien CG, Widman G, Urbach H, et al. **The natural history of Rasmussen's encephalitis.** *Brain* 2002;125:1751–1759
28. Friede RL. *Developmental Neuropathology.* Berlin: Springer-Verlag, 1989
29. Rosenow F, Lüders H. **Presurgical evaluation of epilepsy.** *Brain* 2001;124:1683–1700
30. Wellmer J, von Oertzen J, Schaller C, et al. **Grid electrode localization based on digital photography and 3D-MRI: a method for routine application.** *Epilepsia* 2002;43:1543–1550
31. Kral T, Clusmann H, Urbach H, et al. **Preoperative evaluation for epilepsy surgery (Bonn algorithm).** *Zentralbl Neurochir* 2002;63: 106–110
32. Colombo N, Tassi L, Galli C, et al. **Focal cortical dysplasias: MR imaging, histopathologic, and clinical correlations in surgically treated patients with epilepsy.** *AJNR Am J Neuroradiol* 2003;24: 724–733
33. Spreafico R, Garbelli R, Ferrario A, et al. *Immunocytochemical aspects of focal cortical dysplasia. Syllabus S23–26.* 11th Advanced Course of the ESNR, Ancona, September 13, 2001